IOP Publishing Journal of Physics: Condensed Matter
J. Phys.: Condens. Matter **30** (2018) 155803 (11pp) https://doi.org/10.1088/1361-648X/aab4af

Magnetism of the 35 K superconductor $CsEuFe_4As_4$

Mohammed A Albedah[1,2], Farshad Nejadsattari[1], Zbigniew M Stadnik[1], Yi Liu[3] and Guang-Han Cao[3]

[1] Department of Physics, University of Ottawa, Ottawa, Ontario, K1N 6N5, Canada
[2] Department of Physics, Majmaah University, PO Box 1712, Zulfi, Saudi Arabia
[3] Department of Physics, Zhejiang University, Hangzhou 310027, People's Republic of China

E-mail: stadnik@uottawa.ca

Received 16 January 2018, revised 2 March 2018
Accepted for publication 7 March 2018
Published 21 March 2018

Abstract

The results of *ab initio* hyperfine-interaction parameters calculations, and of x-ray diffraction and ^{57}Fe and ^{151}Eu Mössbauer spectroscopy study of the new 35 K superconductor $CsEuFe_4As_4$ are reported. The superconductor crystallizes in the tetragonal space group *P*4/*mmm* with the lattice parameters $a = 3.8956(1)$ Å and $c = 13.6628(5)$ Å. It is demonstrated unequivocally that there is no magnetic order of the Fe magnetic moments down to 2.1 K and that the ferromagnetic order is associated with the Eu magnetic moments. The Curie temperature $T_C = 15.97(8)$ K determined from the temperature dependence of the hyperfine magnetic field at ^{151}Eu nuclei is shown to be compatible with the temperature dependence of the transferred hyperfine magnetic field at ^{57}Fe nuclei that is induced by the ferromagnetically ordered Eu sublattice. The Eu magnetic moments are shown to be perpendicular to the crystallographic *c*-axis. The temperature dependence of the principal component of the electric field gradient tensor, both at Fe and Eu sites, is well described by a $T^{3/2}$ power-law relation. Good agreement between the calculated and measured hyperfine-interaction parameters is observed. The Debye temperature of $CsEuFe_4As_4$ is found to be 295(3) K.

Keywords: ^{57}Fe and ^{151}Eu Mössbauer sepctroscopy, ferromagnet, electric quadrupole splitting, Debye temperature

(Some figures may appear in colour only in the online journal)

1. Introduction

*Ae*AFe_4As_4 (*Ae* = Ca, Sr, Eu and *A* = K, Rb, Cs) compounds, discovered in 2016, are a new iron-based class of superconductors with the critical temperature T_c in the range 31.6–36.8 K [1–4]. Unlike in solid solutions, such as intensively studied $(Ba_{1-x}K_x)Fe_2As_2$ or $(Sr_{1-x}Na_x)Fe_2As_2$, the *Ae* and *A* atoms in *Ae*AFe_4As_4 occupy the crystallographically inequivalent positions, which changes the space group from *I*4/*mmm* to *P*4/*mmm*. The crystal structure of these new superconductors consists of the *Ae* and *A* layers alternately stacked along the crystallographic *c* axis between the Fe_2As_2 slabs. Thus, these fully ordered, stoichiometric iron-based superconductors offer a unique opportunity to study, among other things, the relation between superconductivity and possible long-range magnetic order.

The new superconductor $CsEuFe_4As_4$ with $T_c = 35.1$–35.2 K shows a magnetic transition at ~15.0–15.5 K in the magnetic susceptibility data [2, 4]. The magnetic transition at 15.2 K has also been observed in the heat capacity data [4]. The isothermal magnetization measurements allowed it to identify this transition as being ferromagnetic [4]. It has been suggested [4] that ferromagnetism in the $CsEuFe_4As_4$ superconductor results from the ordering of the Eu magnetic moments, which is equivalent to assuming that the Fe atoms carry no magnetic moment. No orientation of the magnetic moment in $CsEuFe_4As_4$ with respect to the crystallographic axes has been established.

The primary goal of this study is to find out whether the magnetic moment in the $CsEuFe_4As_4$ superconductor is associated only with Eu or Fe atoms, or with Eu and Fe atoms, and what is its orientation relative to the crystallographic axes.

 © 2018 IOP Publishing Ltd Printed in the UK

To achieve this goal, ^{57}Fe and ^{151}Eu Mössbauer spectroscopy, which proved to be an excellent tool to investigate local magnetism of Fe-based superconductors [5], supplemented by the first-principles calculations, will be utilized.

2. Experimental and theoretical methods

The polycrystalline sample of composition $CsEuFe_4As_4$ was synthesized by a solid-state reaction method in a vacuum and at high temperatures, as described earlier [3, 4].

An x-ray diffraction measurement was carried out at 298 K in Bragg-Brentano geometry on a PANalytical X'Pert scanning diffractometer using Cu $K\alpha$ radiation in the 2θ range 10–120° in steps of 0.02°. The $K\beta$ line was eliminated by using a Kevex PSi2 Peltier-cooled solid-state Si detector.

The ^{57}Fe and ^{151}Eu Mössbauer measurements [6] were conducted using standard Mössbauer spectrometers operating in the sine mode, with sources ^{57}Co(Rh) and ^{151}Sm(SmF_3) at room temperature, respectively. The Mössbauer source ^{151}Sm(SmF_3) is not a monochromatic source as ^{151}Sm nuclei are located in the SmF_3 matrix at a site of noncubic symmetry. By measuring the ^{151}Eu Mössbauer spectra of a cubic EuSe compound, we determined that the electric quadrupole coupling constant [6] eQ_gV_{zz} (here e is the proton charge, $Q_g = 0.903$ b is the ground-state electric quadrupole moment of the ^{151}Eu nucleus [7], and V_{zz} is the principal component of the electric field gradient (EFG) tensor) in our source is $-3.69(13)$ mm s^{-1}, which is close to the value of -3.6 mm s^{-1} found in ([8]). The precise shape of the source emission line was taken into account in the fits of the ^{151}Eu Mössbauer spectra.

The 14.4 and 21.5 keV γ-rays were detected with a proportional counter. The spectrometers were calibrated with a 6.35-μm-thick α-Fe foil [9] and the spectra were folded. The Mössbauer absorbers consisted of a mixture of powder $CsEuFe_4As_4$ and boron nitride, which was pressed into a pellet that was put into a 8-μm-thick Al disk container to ensure a uniform temperature over the whole absorber. The Mössbauer absorbers were put into a Mössbauer cryostat in which they were kept in a static exchange gas atmosphere at a pressure of $\sim 6\times 10^{-3}$ mbar. The surface densities of the ^{57}Fe and ^{151}Eu Mössbauer absorbers were 20.6 and 37.2 mg cm^{-2}, respectively. They correspond to the effective thickness parameter [6] t_a of $3.33f_a$ and $3.15f_a$, respectively (here f_a is the Debye–Waller factor of the absorber). Since $t_a > 1$, the resonance line shape of the Mössbauer spectra was described using a transmission integral formula [10]. The Mössbauer spectra at temperatures below the magnetic transition temperature were analyzed using a least-squares fitting procedure which entailed calculations of the positions and relative intensities of the absorption lines by numerical diagonalization of the full hyperfine interaction Hamiltonian.

Ab initio magnetic moment and Mössbauer hyperfine-interaction parameter calculations have been performed within the framework of density functional theory using the full-potential linearized augmented-plane-wave plus local orbitals (FP-LAPW + lo) method as implemented in the WIEN2k package [11]. The experimental lattice parameters (a and c) and the atomic position parameters in the space group *P4/mmm* (*vide infra*) were used in the calculations.

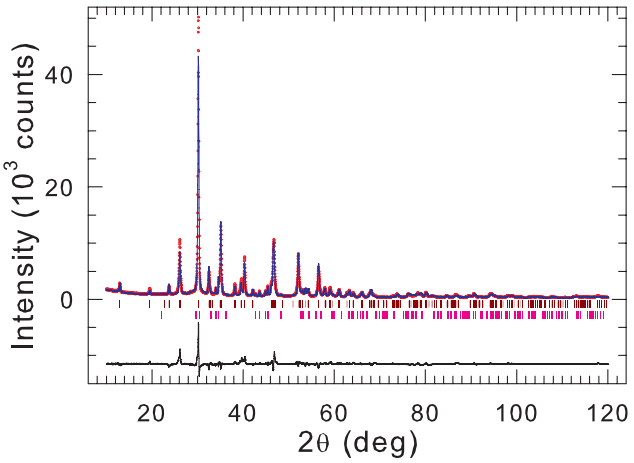

Figure 1. Powder x-ray diffraction pattern of $CsEuFe_4As_4$ at 298 K. The experimental data are denoted by open circles, while the line through the circles represents the results of the Rietveld refinement. The upper set of vertical dark red bars represents the Bragg peak positions corresponding to the $CsEuFe_4As_4$ phase, while the lower set refers to the positions of the impurity phase of FeAs (space group *Pnma*). The lower black solid line represents the difference curve between experimental and calculated patterns.

Table 1. The Rietveld refined atomic positions for the tetragonal $CsEuFe_4As_4$ (space group *P4/mmm*).

Atom	Site	Point symmetry	Occupancy	x	y	z
Cs	1*d*	4/*mmm*	1.0	$\frac{1}{2}$	$\frac{1}{2}$	$\frac{1}{2}$
Eu	1*a*	4/*mmm*	1.0	0	0	0
Fe	4*i*	2 mm.	1.0	0	$\frac{1}{2}$	0.2262(2)
As1	2*g*	4 mm	1.0	0	0	0.3274(2)
As2	2*h*	4 mm	1.0	$\frac{1}{2}$	$\frac{1}{2}$	0.1238(3)

3. Results and discussion

3.1. Structural characterization

The room-temperature powder x-ray diffraction pattern of $CsEuFe_4As_4$ is shown in figure 1. The compound studied crystallizes in the tetragonal space group *P4/mmm* [4]. A Rietveld refinement [12] of the x-ray powder diffraction data was carried out, yielding the lattice parameters $a = 3.8956(1)$ Å and $c = 13.6628(5)$ Å, and the atomic positional parameters that are listed in table 1. We note (figure 1) that the $CsEuFe_4As_4$ specimen contains a second phase of FeAs [13] in the amount of 7.7(2) wt%.

The unit cell and the layered crystal structure of $CsEuFe_4As_4$ are shown in figure 2. The interactions between the Cs, Fe, and As atoms in the compound studied are depicted by various connecting rods. One observes that the layers of Eu atoms are completely isolated from the Fe_4As_4 blocks and that two neighboring Fe_4As_4 blocks are separated by sheets of Cs atoms along the c-direction.

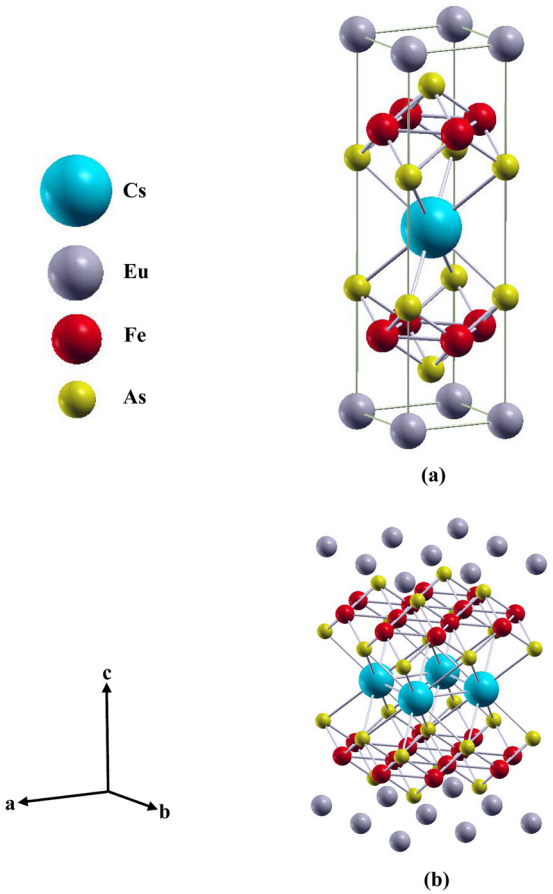

Figure 2. The unit cell (a) and the layered crystal structure (b) of $CsEuFe_4As_4$.

The interatomic distances between various atoms in the $CsEuFe_4As_4$ superconductor play an important role in determining the type of interactions between these atoms. As the dominant physical interaction between the atoms in a solid is electromagnetic in origin, one can conclude that the strength of the Coulomb interaction between the atoms can determine the type of chemical bonding between the constituent atoms of the compound studied. It is seen (figure 2(b)) that the density of atoms within the Fe_4As_4 blocks is greater than that of the Cs and Eu sheets. One thus expects stronger electric interactions to exist within these blocks than within the sheets. This is shown qualitatively in figure 2(b) by a dense network of connecting rods between the Fe and As atoms and the absence of such connecting rods between the Eu atoms.

The $CsFe_4As_4$ units are separated by sheets of Eu atoms (figure 2(b)). The absence of connecting rods between the Eu atoms and the $CsEuFe_4As_4$ units indicates that these units are chemically independent of each other. The Eu sheets act as insulating layers along the *c*-axis, which can be the result of ionic interactions between them and the blocks of Fe_4As_4. Furthermore, the elongated along the *c*-axis tetragonal unit cell rules out the possibility of any strong interaction between the Eu layers. In particular, no magnetic coupling is expected to exist between the Eu atoms along the *c*-direction. One may thus predict that the interatomic interactions between the Eu atoms must occur in the *ab* plane and that a 2D magnetic interaction mechanism, if any, between neighboring Eu atoms in each layer, should exist. Also, the Eu atoms in each layer

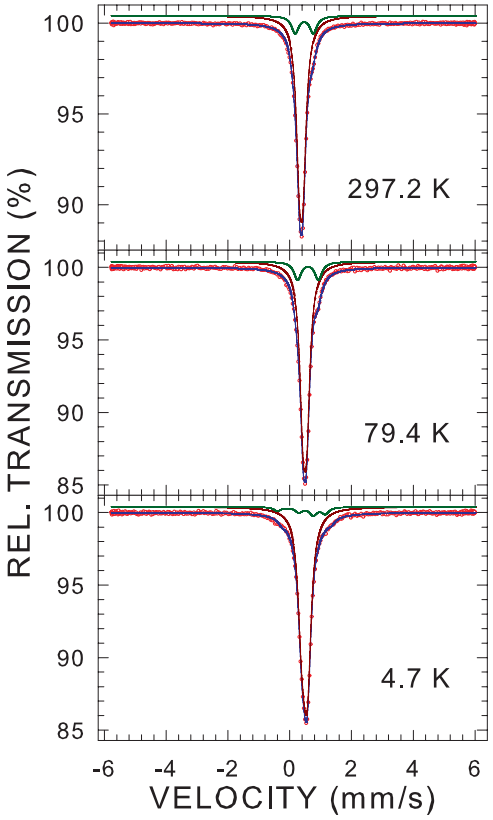

Figure 3. Room-, liquid-nitrogen, and liquid-helium temperature ^{57}Fe Mössbauer spectra of $CsEuFe_4As_4$ measured over a large velocity range and fitted (solid blue lines) with a large spectral area quadrupole doublet at 297.2 and 79.4 K and a Zeeman pattern at 4.7 K (solid dark red lines) due to $CsEuFe_4As_4$, and with a small spectral area doublet at 297.2 and 79.4 K and a Zeeman pattern at 4.7 K (solid dark green lines) due to the FeAs impurity phase, as described in the text. The zero-velocity origin is relative to α-Fe at room temperature.

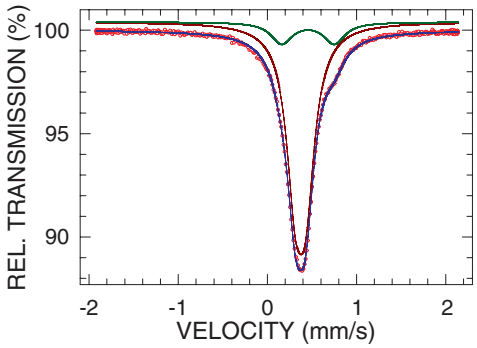

Figure 4. ^{57}Fe Mössbauer spectrum of $CsEuFe_4As_4$ at 297.0 K fitted (solid blue line) with a large spectral area quadrupole doublet due to $CsEuFe_4As_4$ (solid dark red lines) and a small spectral area quadrupole doublet originating from the FeAs impurity phase (solid dark green lines), as described in the text. The zero-velocity origin is relative to α-Fe at room temperature.

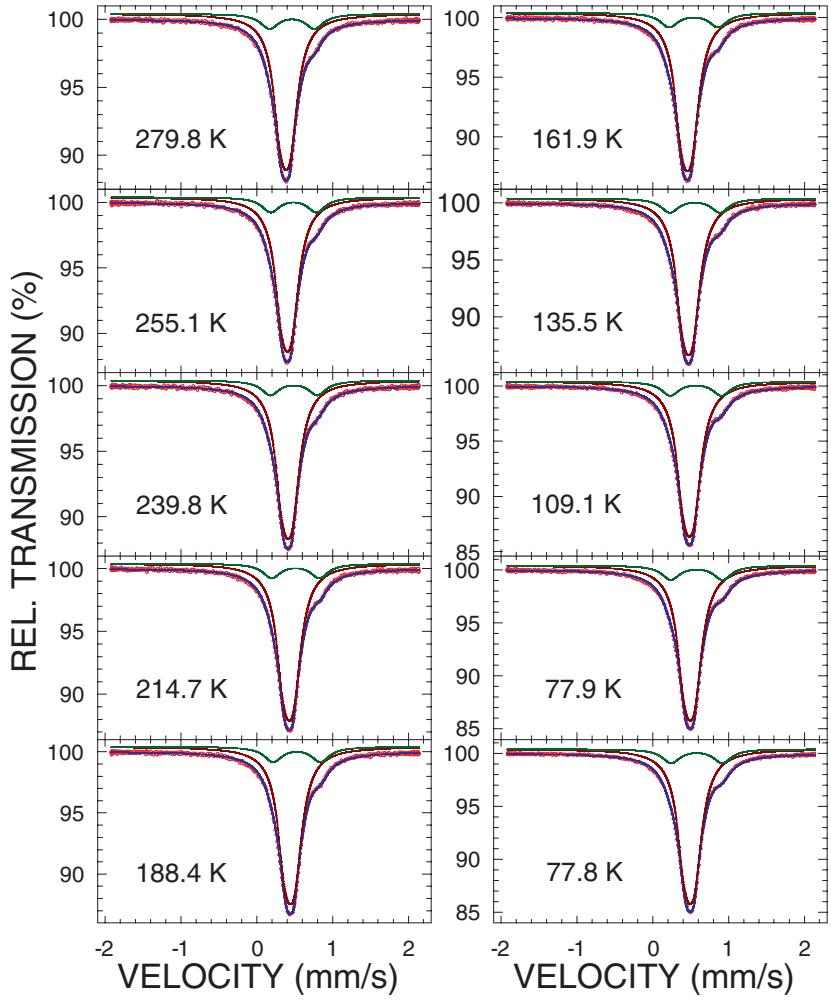

Figure 5. ^{57}Fe Mössbauer spectra of $CsEuFe_4As_4$ at the indicated temperatures fitted (solid blue lines) with a large spectral area quadrupole doublet due to $CsEuFe_4As_4$ (dark red solid lines) and a small spectral area quadrupole doublet originating from the FeAs impurity phase (solid dark green lines), as described in the text. The zero-velocity origin is relative to α-Fe at room temperature.

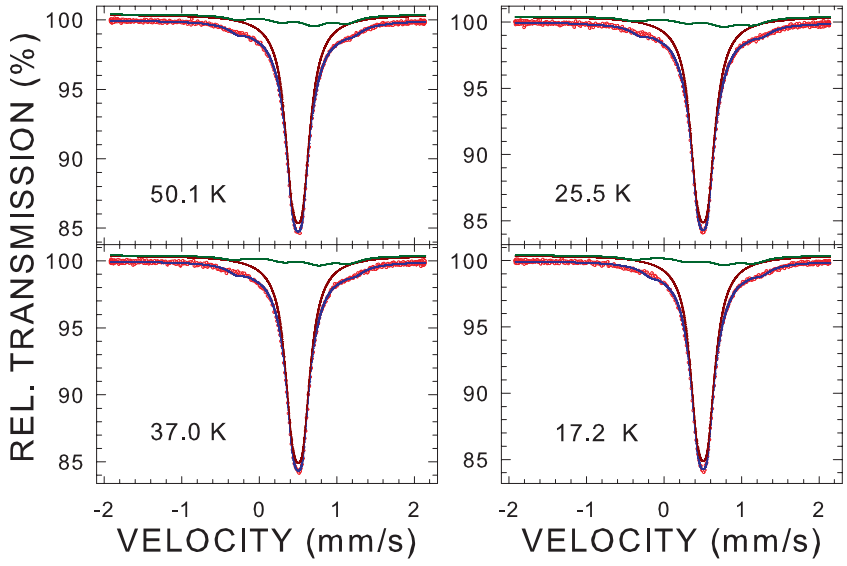

Figure 6. ^{57}Fe Mössbauer spectra of $CsEuFe_4As_4$ at the indicated temperatures fitted (solid blue lines) with a large spectral area quadrupole doublet due to $CsEuFe_4As_4$ (dark red solid lines) and a small spectral area Zeeman pattern originating from the FeAs impurity phase (solid dark green lines), as described in the text. The zero-velocity origin is relative to α-Fe at room temperature.

are themselves isolated from each other, as depicted by the absence of connecting rods between them.

3.2. Calculated magnetic moments and hyperfine interaction parameters

The calculated magnetic moments of the Cs, Eu, Fe, As1, and As2 atoms in the ferromagnetic $CsEuFe_4As_4$ are −0.0060, 6.7057, 1.1229, −0.0709, and −0.0854 μ_B, respectively. It is thus predicted that the magnetism of $CsEuFe_4As_4$ is associated predominantly with the Eu atoms, and to a lesser extent with the Fe atoms. A comparison between the calculated and experimental magnetic moments carried by the Eu and Fe atoms will be made below.

^{57}Fe Mössbauer spectra of a non-magnetic compound, or of a magnetically ordered compound at temperatures above its ordering temperature, yield two important hyperfine-interaction parameters: the quadrupole splitting (the separation between two resonance lines in a ^{57}Fe Mössbauer quadrupole doublet) $\Delta = \frac{1}{2} eQ|V_{zz}|\sqrt{1+\eta^2/3}$, where Q is the electric quadrupole moment of the ^{57}Fe nucleus (0.15 b) [14] and η is the asymmetry parameter, and the isomer shift, δ_0 [6]. For a crystalline compound of known crystal structure, V_{zz}, η, and δ_0 can also be obtained from *ab initio* calculations [15].

The calculated values of V_{zz} and η at the 4*i* site occupied by the Fe atoms (table 1) are 7.142×10^{20} V m^{-2} and 0.7795, respectively. These values correspond to the predicted $\Delta = 0.1222$ mm s^{-1}.

The isomer shift $\delta_0 = \alpha[\rho(0) - \rho_{ref}(0)]$ results from the difference in the total electron density at the Mössbauer nucleus in the compound studied, $\rho(0)$, and in the reference compound, $\rho_{ref}(0)$; α is a calibration constant. In calculating $\rho(0)$, relativistic spin-orbit effects were invoked to account for the possibility of the penetration of the $p_{1/2}$ electrons into the ^{57}Fe nuclei. An α-Fe (with the *bcc* structure and the lattice constant of 2.8665 Å) was chosen as a reference compound. The calculated values of $\rho_{ref}(0)$ and $\rho(0)$ are 15309.905 and 15308.531 (a.u.)$^{-3}$, respectively. Using the calibration constant $\alpha = -0.291$(a.u.)^3(mm s^{-1}), [16] the calculated values of $\rho(0)$ and $\rho_{ref}(0)$ lead to $\delta_0 = 0.400$ mm s^{-1}.

And finally, the calculated hyperfine magnetic field at 0 K (Fermi contact term) at ^{57}Fe nuclei, $H_{hf}(0)$, is −57.7 kOe for the ferromagnetic $CsEuFe_4As_4$.

The analysis of the ^{151}Eu Mössbauer spectra at different temperatures yields similar hyperfine-interaction parameters. The calculated values of V_{zz} and η at the 1*a* site occupied by the Eu atoms (table 1) are -58.017×10^{20} V m^{-2} and 0.0, respectively. The $\eta = 0.0$ value is expected as the point symmetry 4/*mmm* of the 1*a* sites ensures the axially symmetric EFG tensor. The calculated $H_{hf}(0)$ at ^{151}Eu nuclei is 467 kOe for the ferromagnetic $CsEuFe_4As_4$.

3.3. ^{57}Fe Mössbauer spectroscopy

To access the possibility of the presence of a Zeeman pattern resulting from a possible magnetic ordering of the Fe atoms in $CsEuFe_4As_4$, and of a Zeeman pattern due to a magnetically-ordered and Fe-containing impurity phase in the sample

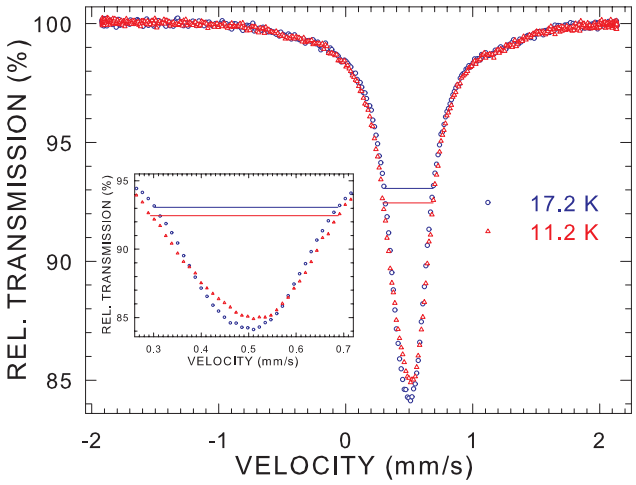

Figure 7. Comparison of the ^{57}Fe Mössbauer spectra of $CsEuFe_4As_4$ at 17.2 and 11.2 K. The inset shows the spectra with the enlarged horizontal and vertical scales. The horizontal bars indicate the full width at half maximum of the 17.2 K spectrum (0.386 mm s^{-1}) and the 11.2 K spectrum (0.396 mm s^{-1}). The zero-velocity origin is relative to α-Fe at room temperature.

studied, the room, liquid-nitrogen, and liquid-helium temperature ^{57}Fe Mössbauer spectra were measured over a large velocity range (figure 3). A visual inspection of these spectra shows the absence of Zeeman patterns corresponding to the main and impurity phases with typical values of the hyperfine magnetic field, H_{hf}. As will be shown in detail below, the large spectral area component of these spectra (figure 3) is due to $CsEuFe_4As_4$ and is in the form of a quadrupole doublet with small Δ at 297.2 and 79.4 K and a Zeeman pattern with very small H_{hf} at 4.7 K. The small spectral area component of the spectra in figure 3 originates from the FeAs impurity phase and is in the form of a quadrupole doublet at 297.2 and 79.4 K and a Zeeman pattern at 4.7 K.

The room-temperature Mössbauer spectrum of $CsEuFe_4As_4$ measured over a small velocity range is shown in figure 4. A feature on the right shoulder of the spectrum indicates the presence of an impurity phase in the compound studied. A satisfactory fit of the spectrum can be obtained with a large spectral area quadrupole doublet component with small Δ that originates from $CsEuFe_4As_4$ and with a small spectral area quadrupole doublet component due to the FeAs impurity phase [17–19].

The Mössbauer spectra of $CsEuFe_4As_4$ at various temperatures down to the liquid nitrogen temperature are shown in figure 5. Their shape is the same as that of the spectrum in figure 4, that is, excellent fits of these spectra could be obtained with two quadrupole doublet components originating from $CsEuFe_4As_4$ and the FeAs impurity phase.

The FeAs impurity component in the Mössbauer spectra of $CsEuFe_4As_4$ at temperatures below the liquid nitrogen temperature (figure 6) is in the form of a complex Zeeman pattern, which indicates that the magnetic ordering temperature of the impurity phase lies in the range 77.8–50.1 K (figures 5 and 6). This agrees with the reported Néel temperature of FeAs (77(1) K in [13] and 69.2(1) K in [19]).

The Mössbauer spectra of $CsEuFe_4As_4$ at 17.2 and 11.2 K are compared in figure 7. One observes that the 11.2 K

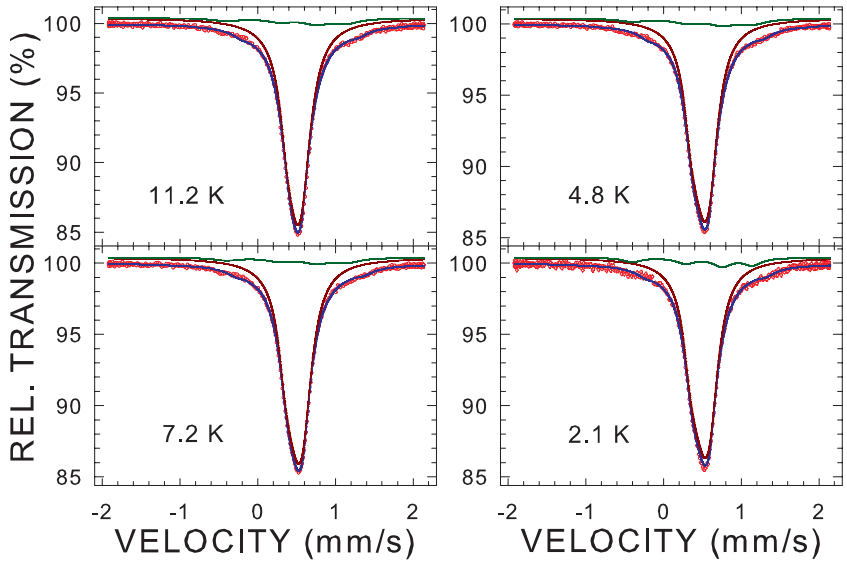

Figure 8. ^{57}Fe Mössbauer spectra of $CsEuFe_4As_4$ at the indicated temperatures fitted (solid blue lines) with a large spectral area Zeeman pattern due to $CsEuFe_4As_4$ (dark red solid lines) and a small spectral area Zeeman pattern originating from the FeAs impurity phase (solid dark green lines), as described in the text. The zero-velocity origin is relative to α-Fe at room temperature.

spectrum is slightly, but visibly broader than the 17.2 K spectrum. This 0.010 mm s^{-1} broadening (figure 7) is the consequence of the appearance at 11.2 K of a very small H_{hf} that is transferred to the ^{57}Fe nuclei from the ferromagnetically ordered Eu sublattice (*vide infra*). It should be stressed that this *transferred* hyperfine magnetic field does not result from the ordering of the Fe sublattice. Its presence constitutes a direct evidence for the ordering of the Eu sublattice. Such a transferred hyperfine magnetic field at a single temperature has been observed for the first time in the $EuFe_2(As_{1-x}P_x)_2$ superconductors [20]. Thus, the Mössbauer spectra at 11.2 K and lower temperatures were fitted (figure 8) with a large spectral area Zeeman pattern component (the value of Δ was fixed in the fit to that obtained from the fit of the 17.2 K spectrum) that originates from $CsEuFe_4As_4$ and with a small spectral area complex Zeeman pattern component that is due to the FeAs impurity phase.

The temperature dependence of the transferred H_{hf} (figure 9), observed here for the first time, was derived from the fits of the spectra in figures 3 and 8. As expected, H_{hf} increases with decreasing temperature. In principle, one could determine from this dependence the ferromagnetic ordering temperature of the Eu sublattice (the Curie temperature), T_C, as the temperature at which $H_{hf} = 0$. However, the paucity of H_{hf} data between 11.2 K and T_C makes it difficult to reliably determine the value of T_C. One can state with certainty (figure 9) that T_C lies between 11.2 and 17.2 K.

The value of T_C derived from the ^{151}Eu Mössbauer spectra is 15.97(8) K (*vide infra*). To show the compatibility of the $H_{hf}(T)$ data in figure 9 with that value of T_C, the $H_{hf}(T)$ dependence was fitted using the phenomenological form [21]

$$H_{hf}(T) = H_{hf}(0)\left[1 - \left(\frac{T}{T_C}\right)^{\alpha}\right]^{\beta}, \qquad (1)$$

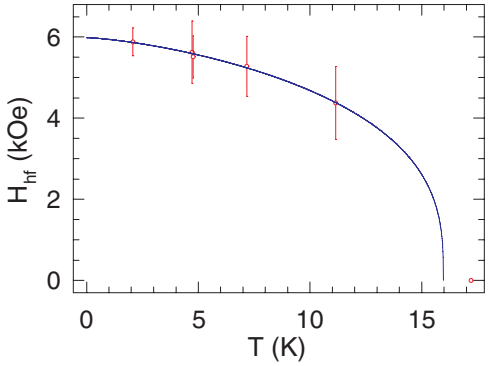

Figure 9. Temperature dependence of the transferred hyperfine magnetic field. The solid line is the fit to equation (1), as explained in the text.

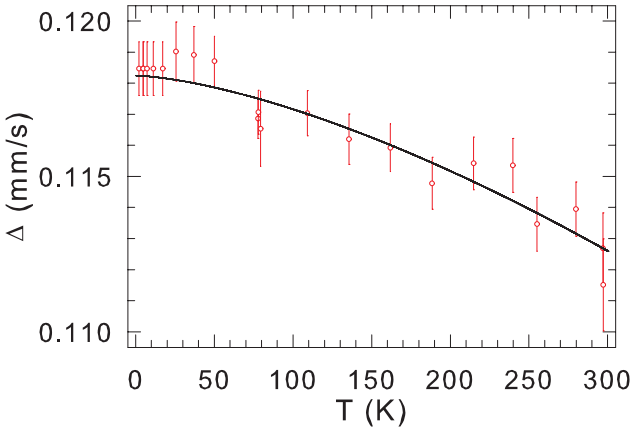

Figure 10. Temperature dependence of the quadrupole splitting. The solid line is the fit to equation (2), as explained in the text.

where $T_C = 15.97$ K, $H_{hf}(0)$ is the value of H_{hf} at 0 K, and α and β are exponents describing the behavior of $H_{hf}(T)$ near 0 K and T_C, respectively. The fit yields $H_{hf}(0) = 5.98(13)$

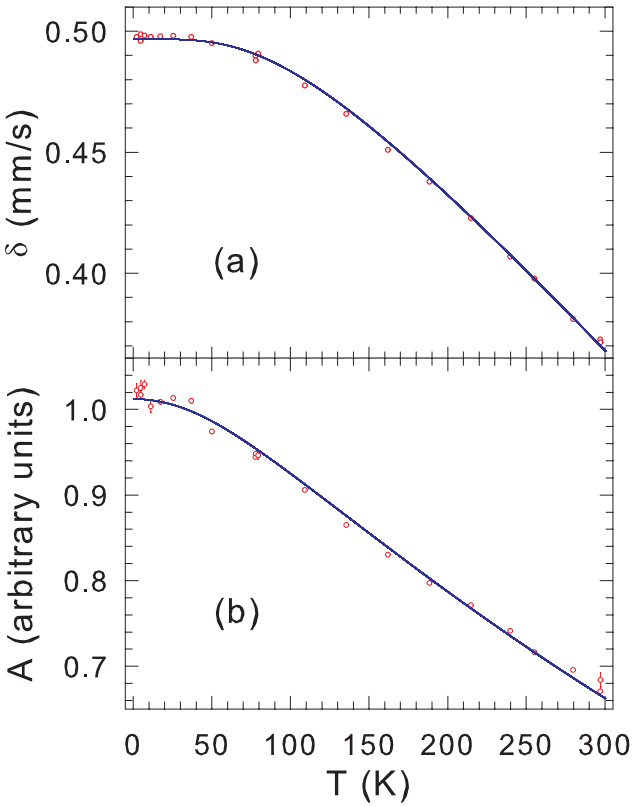

Figure 11. Temperature dependence of (a) the centre shift δ and (b) the absorption spectral area A. The solid lines are the fits to equation (3) in (a) and to equation (5) in (b), as explained in the text.

kOe, $\alpha = 1.39(38)$, and $\beta = 0.33(6)$. The values of α and β found here are comparable to those obtained for other compounds [22–24].

The calculations predict a non-zero, but the small value of $|H_{\rm hf}(0)|$ at the ^{57}Fe nuclei and of the magnetic moment carried by the Fe atoms (*vide supra*). This is at variance with the experimentally observed zero value of the intrinsic, i.e. not transferred, $H_{\rm hf}$ down to 2.1 K, and consequently zero-value of the ordered Fe magnetic moment.

Figure 10 shows the temperature dependence of Δ obtained from the fits of the spectra in figures 3–6 and 8. A small increase of Δ with decreasing temperature is observed. Such a temperature dependence of Δ has been observed in many metallic systems [25–27]. It is well described by the empirical equation

$$\Delta(T) = \Delta(0)\left(1 - BT^{3/2}\right), \tag{2}$$

where $\Delta(0)$ is the value of Δ at 0 K and B is a constant. The fit of the $\Delta(T)$ data (figure 10) to equation (2) gives $\Delta(0) = 0.1182(4)\,\text{mm s}^{-1}$ and $B = 9.20(1.47) \times 10^{-6}\,\text{K}^{-3/2}$. The value of B is similar to that found for other compounds [25–27]. The value of $\Delta(0)$ is very close to the calculated value of $0.1222\,\text{mm s}^{-1}$.

The temperature dependence of the centre shift, δ, that was obtained from the fits of the spectra in figures 3–6 and 8, is shown in figure 11(a). The centre shift at temperature T, $\delta(T)$, consists of two terms

$$\delta(T) = \delta_0 + \delta_{\rm SOD}(T), \tag{3}$$

where δ_0 is the intrinsic, temperature-independent isomer shift and $\delta_{\rm SOD}(T)$ is the second-order Doppler (SOD) shift which depends on the lattice vibrations of the Fe atoms [6]. The latter contribution can be expressed in terms of the Debye approximation of the lattice vibrations as

$$\delta_{\rm SOD}(T) = -\frac{9}{2}\frac{k_{\rm B}T}{Mc}\left(\frac{T}{\Theta_{\rm D}}\right)^3 \int_0^{\Theta_{\rm D}/T} \frac{x^3 {\rm d}x}{{\rm e}^x - 1}, \tag{4}$$

where $k_{\rm B}$ is the Boltzmann constant, M is the mass of the Mössbauer nucleus, c is the speed of light, and $\Theta_{\rm D}$ is the Debye temperature. The fits of the experimental data $\delta(T)$ (figure 11(a)) to equation (3) gives $\delta_0 = 0.491(1)\,\text{mm s}^{-1}$ and $\Theta_{\rm D} = 399(7)$ K. We note that the experimental value of δ_0 found here is 19% larger than the calculated δ_0.

Another method of finding the Debye temperature from Mössbauer spectra involves determining their spectral area at various temperatures. The temperature dependence of the spectral area A derived from the fits of the Mössbauer spectra in figures 3–6 and 8 is displayed in figure 11(b). The spectral area is proportional to $f_{\rm a}$, which is given in the Debye theory by [6]

$$f_{\rm a}(T) = \exp\left\{-\frac{3}{4}\frac{E_\gamma^2}{Mc^2 k_{\rm B}\Theta_{\rm D}}\left[1 + 4\left(\frac{T}{\Theta_{\rm D}}\right)^2 \int_0^{\Theta_{\rm D}/T} \frac{x{\rm d}x}{{\rm e}^x - 1}\right]\right\}, \tag{5}$$

where E_γ is the energy of the Mössbauer transition. The fit of the experimental dependence $A(T)$ (figure 11(b)) to equation (5) gives $\Theta_{\rm D} = 276(3)$ K. The weighted average of the above two $\Theta_{\rm D}$ values determined from the temperature dependence of two different Mössbaue parameters is 295(3) K.

The value of $\Theta_{\rm D}$ determined from the $A(T)$ data is significantly smaller than the one derived from the $\delta(T)$ data. In fact, the $\Theta_{\rm D}$ values determined from the $A(T)$ data are always smaller than the ones obtained from the $\delta(T)$ data. This results from the way in which $\Theta_{\rm D}$ is calculated. One recalls that $f_{\rm a}$ and $\delta_{\rm SOD}$ are related to the mean-square vibrational displacement $\langle x^2\rangle$ and the mean-square velocity $\langle v^2\rangle$ of the Mössbauer nucleus, respectively [6]. Since $\langle x^2\rangle$ weights the phonon frequency distribution by ω^{-1} while $\langle v^2\rangle$ weights it by ω^{+1} [28], the Θ_D values derived from the $A(T)$ data are necessarily lower than those determined from the $\delta(T)$ data.

3.4. ^{151}Eu Mössbauer spectroscopy

The ^{151}Eu Mössbauer spectra of $CsEuFe_4As_4$ measured over the velocity range $\mp 20\,\text{mm s}^{-1}$ and at temperatures between room- and liquid-nitrogen temperatures are shown in figure 12. The large spectral area component originates from Eu^{2+} ions in $CsEuFe_4As_4$ and is in the form of an unresolved quadrupole octet [6, 29]. The small spectral area component is due to Eu^{3+} ions in an unidentified foreign phase and is in the form of a single line. The Mössbauer spectra of $CsEuFe_4As_4$ measured over the velocity range $\mp 50\,\text{mm s}^{-1}$ and at temperatures

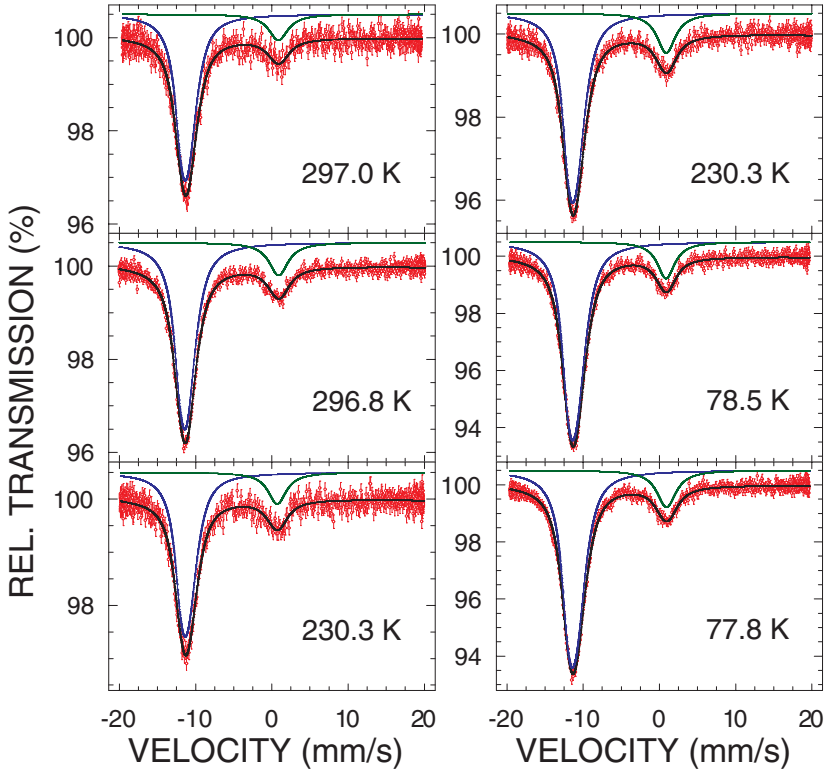

Figure 12. ^{151}Eu Mössbauer spectra of $CsEuFe_4As_4$ at the indicated temperatures fitted (solid black lines) with a large spectral area quadrupole pattern due to $CsEuFe_4As_4$ (blue solid lines) and a small spectral area singlet originating from an impurity phase (solid dark green lines), as described in the text. The zero-velocity origin is relative to the source.

between liquid-nitrogen temperatures and 17.1 K (figure 13) have the same structure as those in figure 12, that is, the studied compound is in the paramagnetic state down to 17.1 K.

The Mössbauer spectrum of $CsEuFe_4As_4$ measured at 8.8 K, that is, below T_C is shown in figure 14. It can be fitted with a large spectral area Zeeman pattern component that originates from $CsEuFe_4As_4$ and a small spectral area single line component due to an impurity phase. The quadrupole coupling constant eQ_gV_{zz} of the Zeeman component was fixed in the fit to the value of -6.660 mm s^{-1} derived from the fit of the 17.1 K spectrum (*vide infra*). The Eu atoms in $CsEuFe_4As_4$ are located at the 1*a* site with the point symmetry 4/*mmm* (table 1), which ensures an axially symmetric (the asymmetry parameter $\eta = 0$) EFG tensor at this site. Also, V_{zz} is parallel to the *c*-axis. The values of the relevant fitted parameters of the Zeeman component are $\delta = -11.220(37)$ mm s^{-1}, $H_{hf} = 223.9(1.0)$ kOe, and the angle between V_{zz} and H_{hf}, $\beta = 87.7(8.1)^\circ$. Since V_{zz} is parallel to the *c*-axis, the value of β shows that the Eu magnetic moment is perpendicular to the *c*-axis, that is, the Eu magnetic moment must lie in the *ab* plane.

As shown above, the determination of the angle β allows one to specify the direction of the Eu magnetic moment with respect to the crystallographic axes. To demonstrate the high reliability of such determination by this hyperfine interaction method, the ^{151}Eu Mössbauer spectra were generated (they include the single-line component contribution due to an impurity), using the hyperfine interaction parameters obtained from the fit of the spectrum in figure 14, for two β values of 0° and 90° that correspond, respectively, to the direction of the Eu magnetic moment being parallel and perpendicular to the *c*-axis (figure 15). One notices a dramatic change in the shape of the generated spectra (figure 15), that is, their strong dependence on the value of β.

Figure 16 shows the spectra at other temperatures below T_C. They were fitted in the same way as the spectrum in figure 14.

The temperature dependence of H_{hf} determined from the fits to the Mössbauer spectra in figures 14 and 16 is shown in figure 17(a). It is usually assumed that the temperature variation of H_{hf} in a magnetically ordered material can be reasonably explained in term of the molecular field model, assuming that H_{hf} is proportional to the sublattice magnetization. In terms of this model, $H_{hf}(T)$ can be expressed as

$$H_{hf}(T) = H_{hf}(0)B_J(x), \tag{6}$$

where $H_{hf}(0)$ is the saturation hyperfine magnetic field, $B_J(x)$ is the Brillouin function defined as

$$B_J(x) = \frac{2J+1}{2J}\coth\left(\frac{2J+1}{2J}x\right) - \frac{1}{2J}\coth\left(\frac{x}{2J}\right) \tag{7}$$

and

$$x = \frac{3J}{J+1}\frac{H_{hf}(T)}{H_{hf}(0)}\frac{T_C}{T}. \tag{8}$$

The fit of the $H_{hf}(T)$ data ((figure 17(a)) to equation (6) with $J = S = 7/2$ (corresponding to a free Eu^{2+} ion) yields $H_{hf}(0) = 272.9(2.8)$ kOe and $T_C = 15.97(8)$ K. The experimental value of $H_{hf}(0)$ is significantly smaller than the calculated Fermi contact value of 467 kOe. This discrepancy can

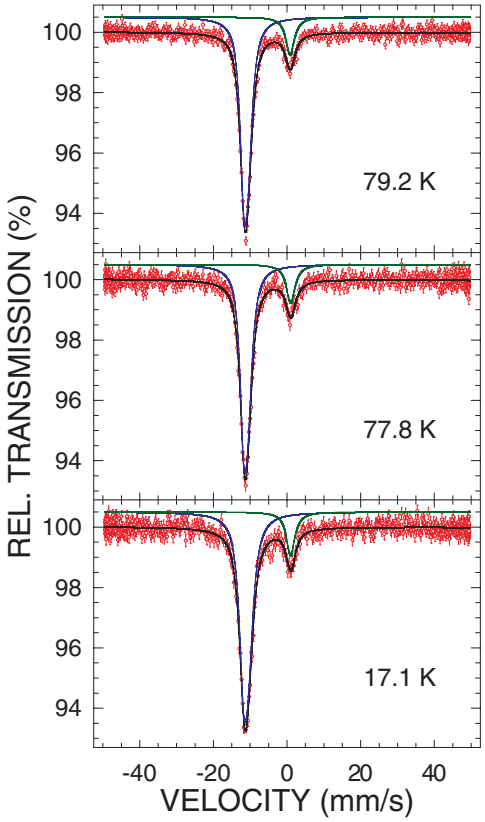

Figure 13. ^{151}Eu Mössbauer spectra of $CsEuFe_4As_4$ at the indicated temperatures fitted (solid black lines) with a large spectral area quadrupole pattern due to $CsEuFe_4As_4$ (blue solid lines) and a small spectral area singlet originating from an impurity phase (solid dark green lines), as described in the text. The zero-velocity origin is relative to the source.

be explained by the fact that the measured hyperfine magnetic field at the ^{151}Eu nuclei is the sum of the Fermi contact term, the contribution from the valence and conduction band electrons, and the contribution due to the neighboring magnetic moments [30]. Clearly, the latter two contributions when added to the Fermi contact term must account for the measured $H_{\rm hf}(0)$.

For ^{151}Eu Mössbauer spectroscopy [29, 30], as opposed to ^{57}Fe Mössbauer spectroscopy [31], there is no simple relation between the measured $H_{\rm hf}(0)$ and the magnetic moment carried by Eu atoms. We note here that the calculated Eu magnetic moment of 6.7057 $\mu_{\rm B}$ is larger than the experimental moment of 5.9 $\mu_{\rm B}$ at 2 K determined from the magnetization measurements [4].

The temperature dependence of the angle β determined from the fits of the spectra in figures 14 and 16 is shown in figure 17(b). One can observe that the β values are close to 90°. This constitutes an experimental proof that the Eu magnetic moments lie in the *ab* plane.

Figure 18(a) shows the temperature dependence of V_{zz} derived from the fits of the spectra in figures 12 and 13. Similarly to the $\Delta(T)$ dependence in figure 10, the magnitude of V_{zz} increases with decreasing temperature. The $V_{zz}(T)$ data can be fitted to an empirical $T^{3/2}$ power-law relation

$$V_{zz}(T) = V_{zz}(0)\left(1 - BT^{3/2}\right), \qquad (9)$$

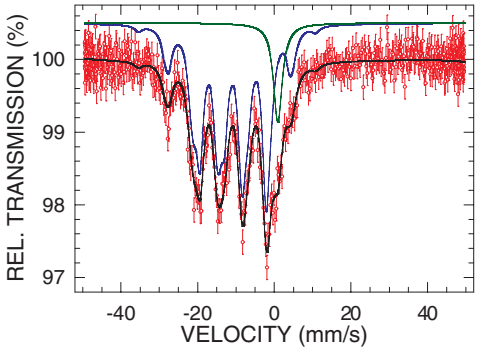

Figure 14. ^{151}Eu Mössbauer spectrum of $CsEuFe_4As_4$ at 8.8 K fitted (solid black line) with a large spectral area Zeeman pattern due to $CsEuFe_4As_4$ (blue solid line) and a small spectral area singlet originating from an impurity phase (solid dark green line), as described in the text. The zero-velocity origin is relative to the source.

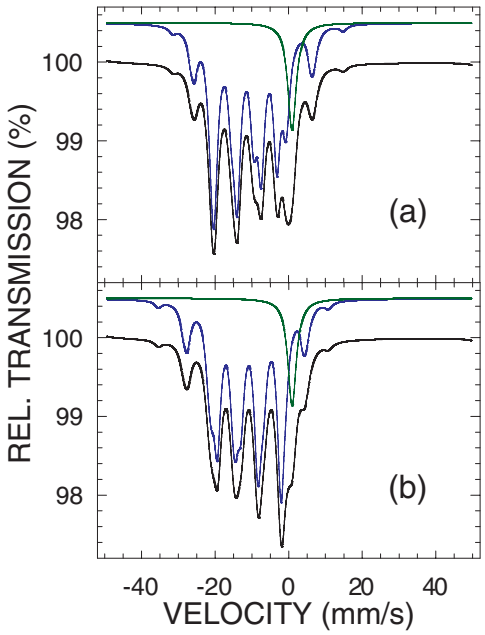

Figure 15. Simulated two-component ^{151}Eu Mössbauer spectra (solid black line). The hyperfine parameters of the single-line component (solid dark green line) and the Zeeman component (blue solid line) are the same as those obtained from the fit of the spectrum in figure 14 with $\beta = 0.0°$ (a) and $\beta = 90°$ (b). The zero-velocity origin is relative to the source.

where $V_{zz}(0)$ is the value of V_{zz} at 0 K and B is a constant. The fit of the $V_{zz}(T)$ data (figure 18(a)) to equation (9) yields $V_{zz}(0) = -0.516(5) \times 10^{22}$ V m^{-2} and $B = 5.28(55) \times 10^{-5}K^{-3/2}$. The experimental value of $V_{zz}(0)$ compares well with the calculated value of -0.580×10^{22} V m^{-2}.

The temperature dependence of δ, that was derived from the fits of the spectra in figures 12–14 and 16, is shown in figure 18(b). The values of $\delta(T)$ prove [29] that at all temperatures the Eu atoms are in the $^8S_{7/2}$ ground state, that is, are divalent. Because of a relatively large scatter and error of the experimental $\delta(T)$ points (figure 18(b)), and of the small rate of temperature change of $\delta_{\rm SOD}$ at high temperatures (-2.76×10^{-4} mm (s·K)$^{-1}$ for ^{151}Eu versus -7.31×10^{-4} mm (s · K)$^{-1}$ for ^{57}Fe), it is not feasible to fit the $\delta(T)$ data to

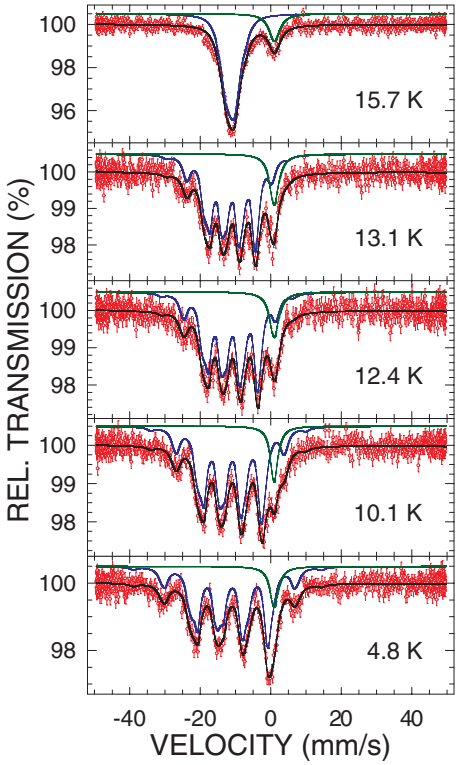

Figure 16. ^{151}Eu Mössbauer spectra of $CsEuFe_4As_4$ at the indicated temperatures fitted (solid black lines) with a large spectral area Zeeman pattern due due to $CsEuFe_4As_4$ (blue solid lines) and a small spectral area singlet originating from an impurity phase (solid dark green lines), as described in the text. The zero-velocity origin is relative to the source.

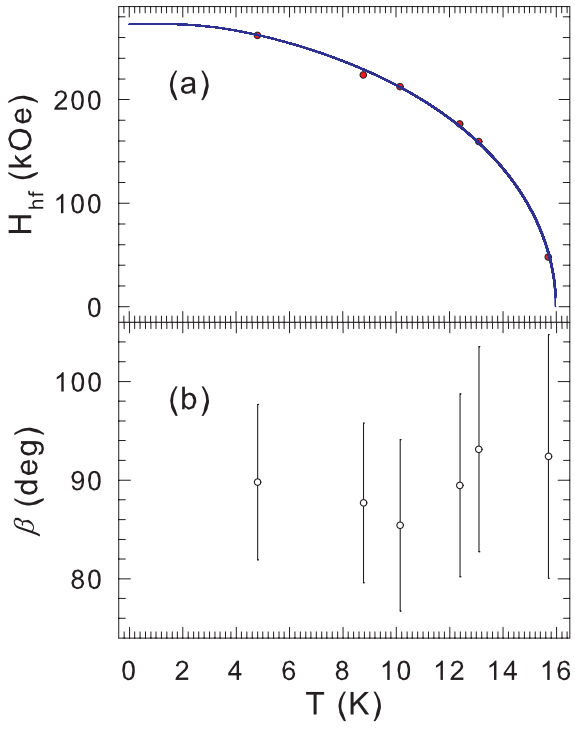

Figure 17. Temperature dependence of the hyperfine magnetic field H_{hf} (a) and the angle β (b) determined from the fits of the spectra in figures 14 and 16. The solid line in (a) is the fit to equation (6), as explained in the text.

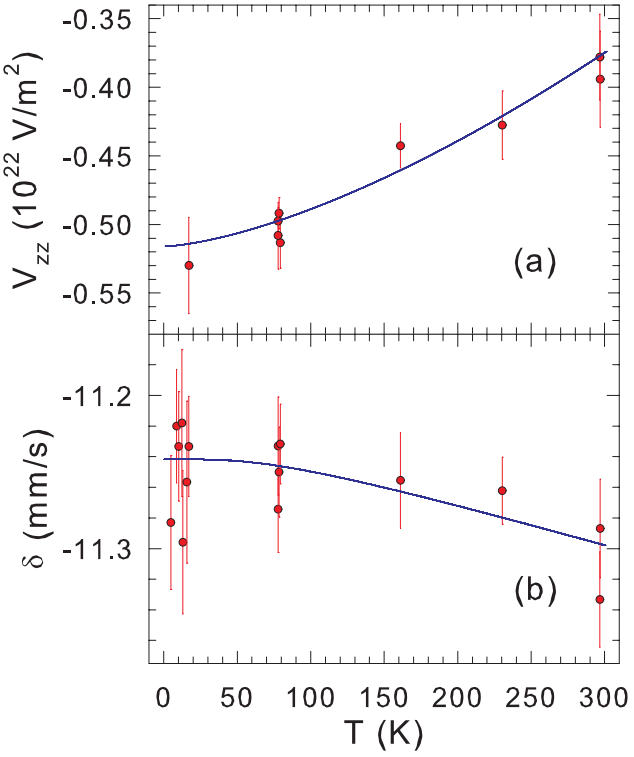

Figure 18. Temperature dependence of the principal component of the electric field gradient tensor V_{zz} derived from the fits of the spectra in figures 12 and 13(a) and of the centre shift δ derived from the fits of the spectra in figures 12–14 and 16. The solid line in (a) is the fit to equation (9), and the solid line in (b) is the variation of $\delta_{SOD}(T)$ calculated for $\Theta_D = 295$ K, as explained in the text.

equation (3) to derive the value of Θ_D. Instead, the temperature variation of δ_{SOD} was calculated for the value of $\Theta_D = 295$ K derived from the ^{57}Fe spectra (solid line in figure 18(b)). The calculated $\delta_{SOD}(T)$ variation approximately accounts for the increase of δ with decreasing temperature.

4. Conclusions

We present the results of *ab initio* hyperfine-interaction parameters calculations, and of x-ray diffraction and ^{57}Fe and ^{151}Eu Mössbauer spectroscopy study of the new 35 K superconductor $CsEuFe_4As_4$. We confirm that the superconductor crystallizes in the tetragonal space group *P4/mmm* with the lattice parameters $a = 3.8956(1)$ Å and $c = 13.6628(5)$ Å. We show that the Fe atoms carry no magnetic moment down to 2.1 K and that the ferromagnetic order is associated with the Eu magnetic moments. We establish that the Curie temperature $T_C = 15.97(8)$ K determined from the temperature dependence of the hyperfine magnetic field at ^{151}Eu nuclei is compatible with the temperature dependence of the transferred hyperfine magnetic field at ^{57}Fe nuclei that is induced by the ferromagnetically ordered Eu sublattice. We find that the Eu magnetic moments are lying in the *ab* plane. We observe that the temperature dependence of the principal component of the electric field gradient tensor is well described by a $T^{3/2}$ power-law relation at both the Fe and Eu sites. Good agreement is found between the calculated and

measured hyperfine-interaction parameters. We determine that the Debye temperature of $CsEuFe_4As_4$ is 295(3) K.

Acknowledgments

This work was supported by the Natural Sciences and Engineering Research Council of Canada (NSERC).

ORCID iDs

Zbigniew M Stadnik https://orcid.org/0000-0002-2785-3930

References

[1] Iyo A, Kawashima K, Kinjo T, Nishio T, Ishida S, Fujihisa H, Gotoh Y, Kihou K, Eisaki H and Yoshida Y 2016 *J. Am. Chem. Soc.* **138** 3410
[2] Kawashima K, Kinjo T, Nishio T, Ishida S, Fujihisa H, Gotoh Y, Kihou K, Eisaki H, Yoshida Y and Iyo A 2016 *J. Phys. Soc. Japan* **85** 064710
[3] Liu Y, Liu Y-B, Jiang H, Wang Z-C, Ablimit A, Jiao W-H, Tao Q, Feng C-M, Xu Z-A and Cao G-H 2016 *Phys. Rev.* B **93** 214503
[4] Liu Y, Liu Y-B, Chen Q, Tang Z-T, Jiao W-H, Tao Q, Xu Z-A and Cao G-H 2016 *Sci. Bull.* **61** 1213
[5] Pissas M, Sanakis Y, Psycharis V, Simopoulos A, Devlin E, Ren Z-A, Shen X-L, Che G-C and Zhao Z-X 2008 *Supercond. Sci. Technol.* **21** 115015
Albedah M A, Nejadsattari F, Stadnik Z M, Wang Z-C, Wang C and Cao G-H 2017 *J. Alloys Compd.* **695** 1128
[6] Greenwood N N and Gibb T C 1971 *Mössbauer Spectroscopy* (London: Chapman and Hall)
Gütlich P, Bill E and Trautwein A 2011 *Mössbauer Spectroscopy and Transition Metal Chemistry* (Berlin: Springer)
[7] Tanaka Y, Steffen R M, Shera E B, Reuter W, Hoehn M V and Zumbro J D 1984 *Phys. Rev.* C **29** 1830
[8] Nowik I and Felner I 1986 *Hyperfine Interact.* **28** 959
[9] Cali J P (ed) 1971 *Certificate of Calibration, Iron Foil Mössbauer Standard* vol 1541 (Washington, DC: US GPO)
[10] Margulies S and Ehrman J R 1961 *Nucl. Instrum. Methods* **12** 131
Shenoy G K, Friedt J M, Maletta H and Ruby S L 1974 *Mössbauer Effect Methodology* vol 10, ed I J Gruverman *et al* (New York: Plenum) p 277
[11] Blaha P, Schwartz K, Madsen G, Kvasnicka D and Luitz J 1999 *WIEN2k, An Augmented Plane Wave Plus Local Orbitals Program for Calculating Crystal Properties* ed K Schwarz (Austria: Technical Universität Wien)
Nejadsattari F, Wang P, Stadnik Z M, Nagata Y and Ohnishi T 2017 *J. Alloys Compd.* **725** 1098
[12] Young R A 1993 *The Rietveld Method* (Oxford: Oxford University Press)
[13] Selte K, Kjekshus A and Andersen A F 1972 *Acta Chem. Scand.* **26** 3101
[14] Martínez-Pinedo G, Schwerdtfeger P, Caurier E, Langanke K, Nazarewich W and Söhnel T 2001 *Phys. Rev. Lett.* **87** 062701
[15] Blaha P 2010 *J. Phys.: Conf. Ser.* **217** 012009
[16] Wdowik U D and Reubenbauer K 2007 *Phys. Rev.* B **76** 155118
[17] Kulshreshtha S K and Raj P 1979 *J. Phys. F: Met. Phys.* **9** 2253
[18] Häggström L, Gustavsson-Seidel A and Fjellvåg H 1989 *Europhys. Lett.* **9** 87
[19] Błachowski A, Ruebenbauer K, Żukrowski J and Bukowski Z 2014 *J. Alloys. Compd.* **582** 167
[20] Nowik I, Felner I, Ren Z, Cao G H and Xu Z A 2011 *J. Phys.: Condens. Matter* **23** 065701
[21] Blundell S J, Steer C A, Pratt F L, Marshall I M, Hayes W and Ward R C C 2003 *Phys. Rev.* B **67** 224411
[22] Baker P J, Franke I, Lancaster T, Bundell S J, Kerslake L and Clarke S J 2009 *Phys. Rev.* B **79** 060402
[23] Baker P J, Lewtas H J, Bundell S J, Lancaster T, Franke I, Hayes W, Pratt F L, Bohatý L and Becker P 2010 *Phys. Rev.* B **81** 214403
[24] Li Z, Fang Y, Ma X, Pang H and Li F 2011 *Phys. Rev.* B **84** 134509
[25] Albedah M A, Nejadsattari F, Stadnik Z M and Przewoźnik J 2015 *J. Alloys Compd.* **619** 839
[26] Stadnik Z M, Wang P, Wang H-D, Dong C-H and Fang M-H 2013 *J. Alloys Compd.* **561** 82
[27] Stadnik Z M and Wang P 2006 *J. Phys.: Condens. Matter* **18** 8383
[28] Housley R M and Hess F 1966 *Phys. Rev.* **146** 517
[29] Grandjean F and Long G L 1989 *Mössbauer Spectroscopy Applied to Inorganic Chemistry* vol 3, ed G J Long and F Grandjean (New York: Plenum) p 513
[30] Albedah M A, Al-Qadi K, Stadnik Z M and Przewoźnik J 2014 *J. Alloys Compd.* **613** 344
[31] Nejadsattari F, Stadnik Z M, Przewoźnik J and Buschow K H J 2015 *Physica* B **477** 113